A Study on the Estimation Method for Underground Structure Using Microtremors and its Application to the Osaka Plain

K. Tobita
Graduate School of Engineering, Kyoto University, Kyoto, Kyoto, Japan

H. Kawase & S. Matsushima
DPRI, Kyoto University, Japan

15 WCEE
LISBOA 2012

SUMMARY
It is essential to evaluate an underground structure properly and validate previously proposed ground structure models based on the geological data and boring exploration data with the observation of ground shaking for extensive and highly precise estimation of strong ground motion in urban areas. In this study, we observed microtremors in the southern part of the Osaka Plain, Japan where detailed geological information are comparatively less than the other areas of the Osaka Plain. We calculated H/V spectral ratio from observed microtremors data and compared predominant peak frequencies and amplitudes at these frequencies of the H/V spectral ratio with those calculated theoretically from our initial model. We searched for the better 1-D structures at each site based on these predominant frequencies and amplitudes. As a result we identified the modified ground structures for each observation point along the two east-west lines in the southern part of the Osaka Plain.

Keywords: Microtremors, H/V Spectral Ratio, Osaka Plain

1. INTRODUCTION

Japan is one of the most seismologically active areas in the world and most of the large cities in Japan are on the alluvial plains. Especially, it is said that western Japan is now in the decades when inland faults are active until the anticipated Tonankai and Nankai subduction earthquakes in the next 30 to 50 years. There are also many inland earthquakes in the eastern part of Japan triggered by the 2011 Great Tohoku earthquake. In addition, surface geology has a great effect on the characteristics of the ground motion observed on these alluvial plains. Therefore, it is essential to evaluate an underground structure properly and validate the previously proposed ground structure models based on the geological data and boring exploration data with the observation data of ground shaking for extensive and highly precise estimation of strong ground motion in urban areas.

Under the initiative of The Headquarters for Earthquake Research Promotion, many subsurface structure models of the Osaka Plain have been proposed and some estimation of strong ground motion with those models considering the source rupture process has been reported. However, the southern part of the Osaka Plain has comparatively less detailed geological information today than other areas of the Osaka Plain. In addition, estimation of strong ground motion up to high frequency range taking in account of effects of surface geology has not been practiced yet.

Therefore, in this study, we observed microtremors in the southern part of the Osaka Plain where detailed geological information are comparatively less than the other areas of the Osaka Plain. We calculated predominant peak frequencies of the ground by using H/V spectral ratio from observed microtremors data and compared these frequencies and amplitudes at these frequencies with those calculated theoretically from our initial model consisting of the model proposed by National Institute of Earth Science and Disaster Prevention (NIED) for the deeper part and National Institute of Advanced Industrial Science and Technology (AIST) for the shallower part. We compared the observed and theoretical predominant frequencies and amplitudes at these frequencies calculated from

H/V spectral ratios and searched for the better 1-D structures at each site based on those predominant frequencies and amplitudes using several different approaches.

2. OUTLINE OF MICROTREMOR MEASUREMENT

We observed microtremors in the southern part of the Osaka Plain. We chose two east-west lines that are 5km apart and go across Uemachi and Ikoma fault zones. Each line has 22 observation points which are located at intervals of 1km, so we observed microtremors at 44 observation points in total. We also observed at two K-NET (Kinoshita, 1998) sites and one KiK-net (Aoi *et al.*, 2000) site, namely, OSK006(Sakai), OSK007(Habikino), and OSKH03(Taishi) as shown in Fig. 2.1. Fig. 2.1 shows the map of Osaka with the observation area and the distribution of observation points.

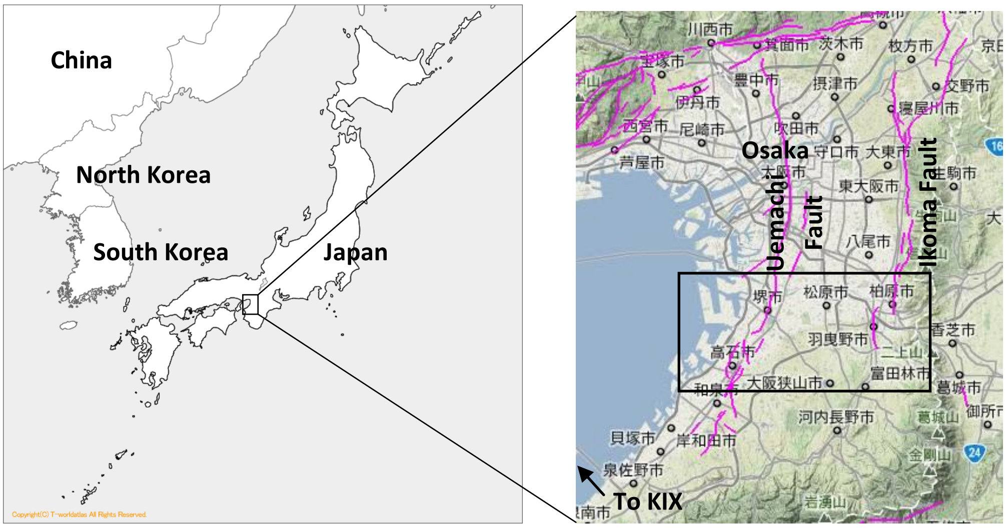

(a) Map of Osaka and the location of the observation area

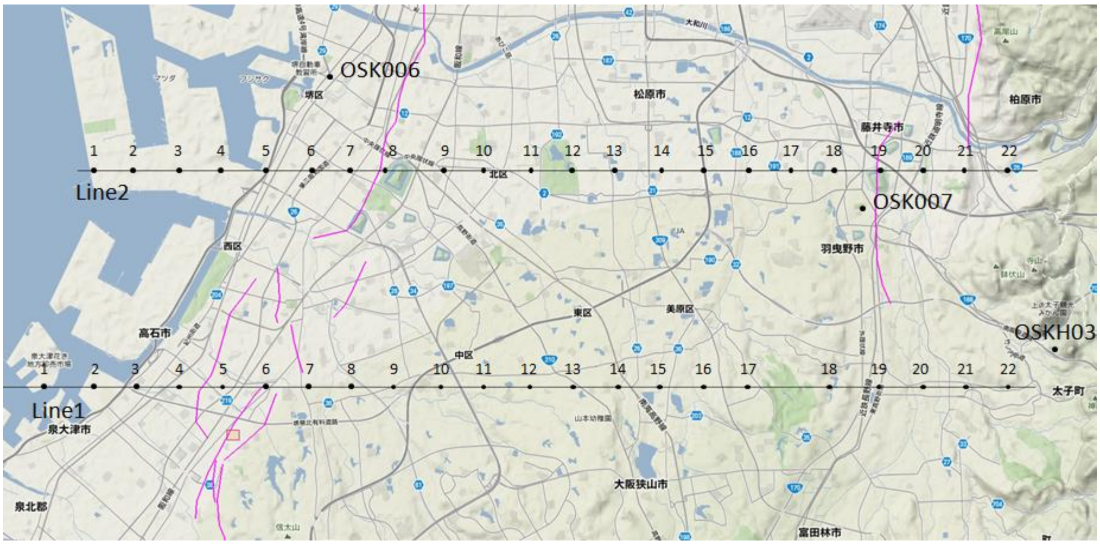

(b) The observation area and the distribution of observation points

Figure 2.1. (a) Map of Osaka with the location of the observation area which is surrounded by black line, and (b) the observation area and the distribution of observation points. Dots with numbers on survey lines Line 1 and 2 denote the microtremors observation points, dots with 6 letter codes denote the strong motion observation stations deployed by NIED and pink lines show the location of known active faults(after Japan Seismic Hazard Information Station (J-SHIS))

Microtremor measurements were conducted at least twice in sets of 15 minutes at each observation point with an acceleration seismograph SMAR-6A3P. Sampling frequency was 100Hz and the signal was amplified 500 times but declined to 200 times when the observation points were close to artificial noise (e.g. local traffic, factories). Then we calculated H/V spectral ratio, or NS/UD and EW/UD spectral ratio, with acceleration time history data gained from microtremor measurements. For conventional H/V spectral ratio studies, two horizontal components are averaged, but in this study we separately use NS/UD and EW/UD to check the directional dependency of H/V spectral ratios as seen in other studies (e.g. Matsushima *et al*., 2012).

In this paper, the code for the observation points such as osk1-2 stands for point No.2 on Line 1 as shown in Fig. 2.1. After three microtremor measurements, there were some observation points left at which amplitudes at predominant frequencies in the H/V spectral ratio were considerably small or judgments of the predominant frequencies in the H/V spectral ratio were comparatively difficult. This may imply that at those observation points, there is no boundary that has large impedance contrast.

3. RESULT OF MICROTREMOR MEASUREMENT

3.1. Waveform Processing of Microtremors

First, we cut off all the acceleration time history data of microtremors into 40.96-second data with overlap of 50 %. Then, we used the following formulas in waveform processing of microtremors.

$$S_{XX}(\omega) = \frac{2}{NT}\sum_{i=1}^{N}\left\{X_i(\omega)X_i^*(\omega)\right\} \tag{3.1}$$

$$S_{YY}(\omega) = \frac{2}{NT}\sum_{i=1}^{N}\left\{Y_i(\omega)Y_i^*(\omega)\right\} \tag{3.2}$$

$$R(\omega) = \sqrt{\frac{S_{YY}(\omega)}{S_{XX}(\omega)}} \tag{3.3}$$

where $S_{XX}(\omega)$ and $S_{YY}(\omega)$ are power spectra, ω is circular frequency, N is the number of data, T is the duration time, $X_i(\omega)$ are finite Fourier transform of vertical microtremors records X_i by using Fast Fourier Transform(FFT), $Y_i(\omega)$ are finite Fourier transform of horizontal microtremors records Y_i by using FFT, $X_i^*(\omega)$ and $Y_i^*(\omega)$ are conjugate complex numbers of $X_i(\omega)$ and $Y_i(\omega)$ respectively, and $R(\omega)$ is the spectrum ratio of $S_{XX}(\omega)$ and $S_{YY}(\omega)$.

We used first and second peak frequencies to determine the first and second predominant frequencies in the microtremors H/V spectral ratio. When the predominant frequencies were not clear, comparing NS/UD spectral ratio with EW/UD spectral ratio and checking predominant frequencies in horizontal Fourier spectrum helped our decision.

3.2. Result of Microtremor Measurement

Fig. 3.1 shows comparison of NS/UD spectral ratio with EW/UD spectral ratio gained from microtremors measurement at one typical observation point. We can see two peak predominant frequencies at around 0.2Hz and 1.5Hz.

Fig. 3.2 shows distributions of predominant frequencies for points on Line 1 and Line 2. The west side of the Osaka Plain is the Osaka bay and the plain faces the mountains in the eastern part of it, so it can be assumed that in general the subsurface structure gets shallower, or predominant frequencies get higher from west to east. For Line 1 in Fig. 3.2a, the first peak frequency gets slightly higher toward east at the eastern end of the line and the second peak frequency in general gets higher toward east, although it has fluctuations locally. For Line 2 in Fig. 3.2b, the first peak frequency gets slightly higher toward east at the eastern end of the line and the second peak frequency is comparatively stable between osk2-1 and osk2-18 but changes rapidly between osk2-19 and osk2-22, so it can be said the subsurface structures around these points are changing locally.

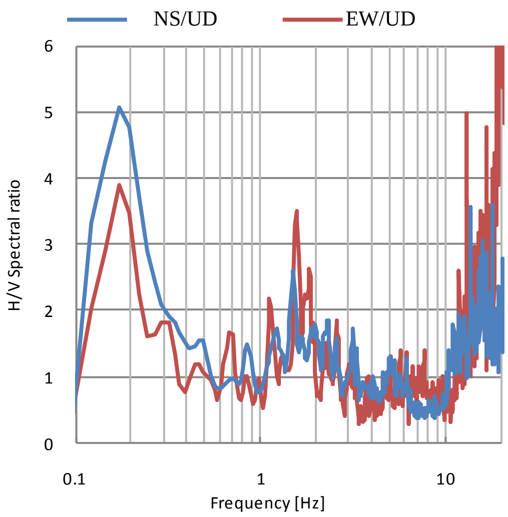

Figure 3.1. Comparison of NS/UD spectral ratio with EW/UD spectral ratio at osk2-13

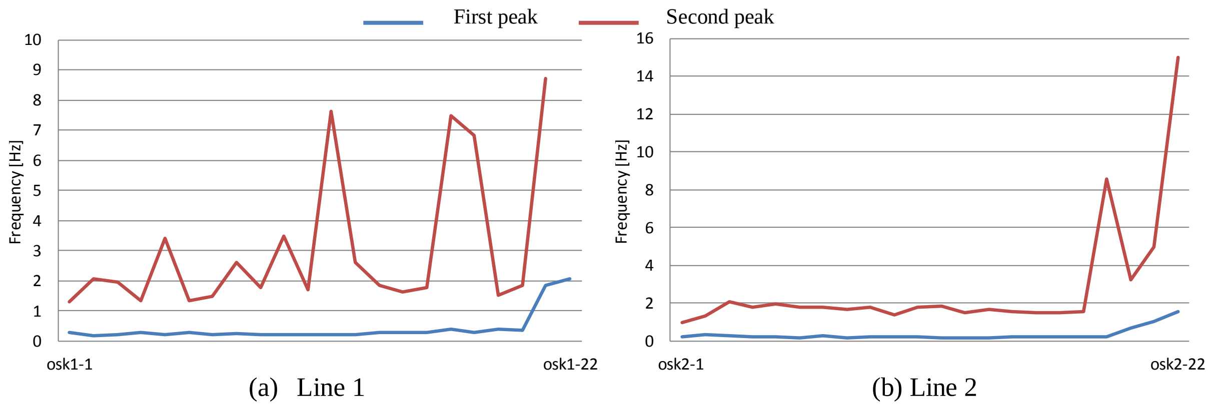

Figure 3.2. Distribution of predominant frequencies of first and second peaks for points on (a) Line 1 and (b) Line 2 in Fig. 2.1(b)

4. VALIDATION FOR THEORETICAL CALCULATION AND IDENTIFICATION APPROACH

We used the code by Dr. Sánchez-Sesma which calculates theoretical microtremor H/V spectral ratio for a given subsurface structure model (Sánchez-Sesma *et al.*, 2008; Sánchez-Sesma *et al.*, 2011).

We calculated theoretical H/V spectral ratio from the subsurface structure models of 3 strong ground motion stations of NIED. By comparing the theoretical H/V spectral ratio with the observed, we tried to validate the theoretical calculation scheme and our estimation approach for a subsurface structure. It is important that we have a good initial model at each strong ground motion station. We add a shallow subsurface structure model from P-S logging surveys at each strong ground motion station into a deeper subsurface structure model proposed by NIED and used the newly-constituted model in the theoretical calculation.

Fig. 4.1 shows comparison of theoretical and observed H/V spectral ratios at the three strong ground motion stations. At OSK006, predominant frequencies and the amplitude of the peak in both H/V spectral ratios are almost same. At OSK007, first peak frequencies are similar, but the amplitude at second peak frequency for theory is considerably small. This can be the result that OSK007 is located in the western side of Ikoma fault zone which are reverse faults and the bedrock in the eastern part of Ikoma fault zone is uplifted because of the movement of the fault and the site has an effect of lateral heterogeneity of the subsurface structure. At OSKH03, observed data is not stable and observed and theoretical H/V spectral ratios are not in good match as those at other stations. This can be due to the fact that OSKH03 is in the mountains and influenced by effects of topography and lateral heterogeneity of the subsurface structure.

As a result, we made sure that both H/V spectral ratios gained from theoretical calculation and observation records were roughly similar except OSKH03 which is in the mountains. Therefore it is shown that if the observation point is on alluvial plains we are able to identify a modified subsurface structure close to the real structure at an point by calculating H/V spectral ratio from an initial subsurface structure model based on previously proposed studies with our theoretical calculation program and fitting the H/V spectral ratio to the observed H/V spectral ratio

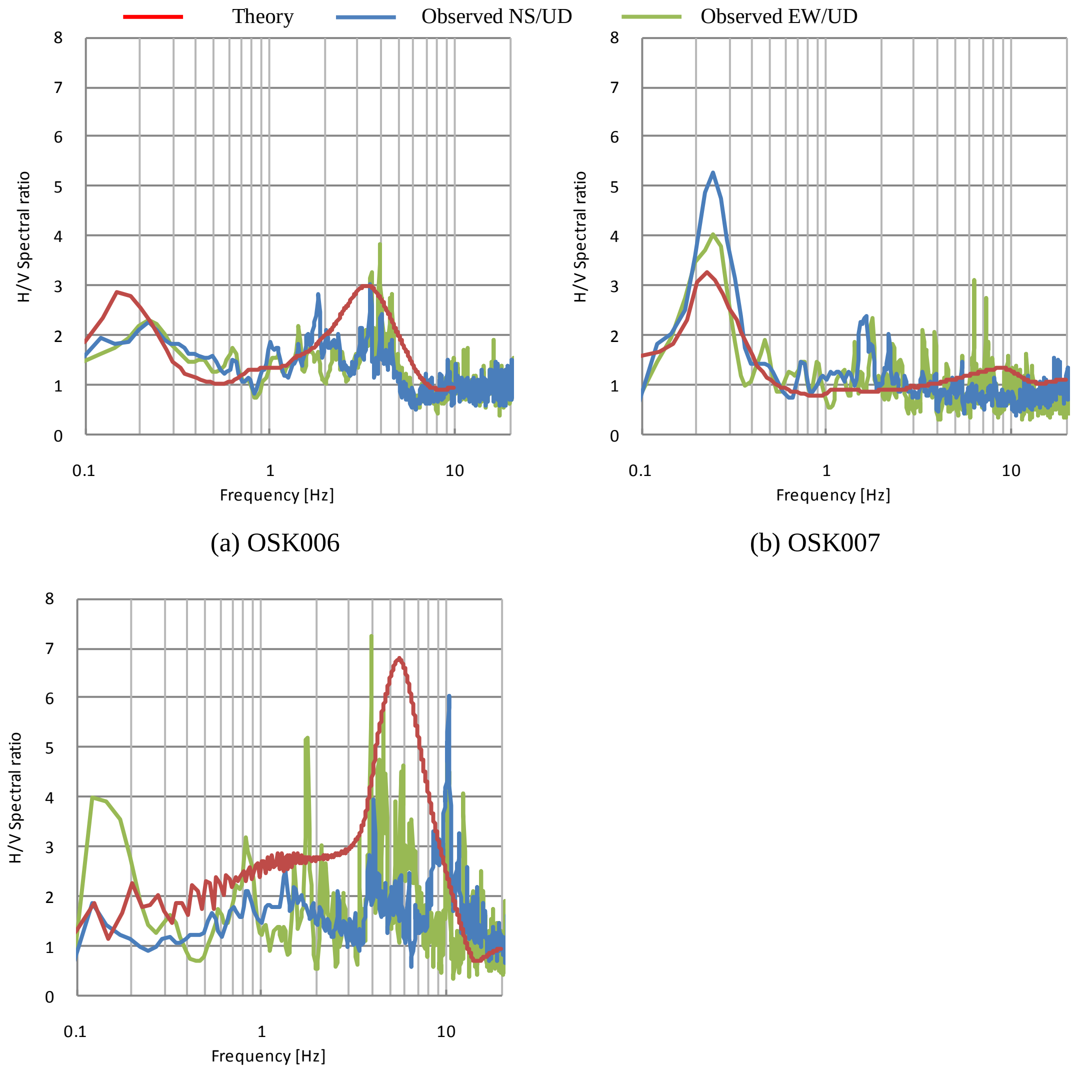

(a) OSK006 (b) OSK007

(c) OSKH03

Figure 4.1. Comparison of H/V spectral ratios for theory and observed at (a) OSK006, (b) OSK007, (c) OSKH03

5. ESTIMATION OF UNDERGROUND STRUCTURES

We need an initial model for a subsurface structure to calculate theoretical H/V spectral ratio. We used an initial model consisting of models proposed by NIED (J-SHIS, 2011) for the deeper part and AIST (Sekiguchi, 2005; Yoshida, 2010) for the shallower part. We added the AIST model into the most surface layer of the NIED model and calculated theoretical H/V spectral ratio with it. In identifying a modified subsurface structure, we used the following two procedures.

Firstly we identified only thickness of underground layers. We judged that the first peak frequency among predominant frequencies reflects the deeper subsurface structure and the second peak reflects the shallower subsurface structure. Then according to the fact that resonant phenomena follow 1/4 wavelength law, we multiplied the ratio of the first peak frequencies of H/V spectral ratios of observed and theory for the initial model to the whole layer thickness of the deeper subsurface structure of the initial model. Similarly, we multiplied the ratio of the second peak frequencies of H/V spectral ratios of observed and theory for the initial model to the whole layer thickness of the shallower subsurface structure of the initial model.

Fig. 5.1 shows comparison of H/V spectral ratios for observed data, initial model, and modified model at two typical observation points. At osk2-11, the predominant frequencies and the amplitudes at the frequencies for observed and modified models correspond well. However at osk1-4 the predominant frequencies for the two correspond but the shape of H/V spectral ratios for the two are considerably different.

Fig. 5.2 and 5.3 show the sections of the shallower and deeper subsurface structures for the initial and modified models of Line 2. As a result, the sections, especially of the deeper subsurface structures for the modified models are considerably different from our expectation that the subsurface structure in the Osaka Plain should be getting deeper toward west from east on Line 2 in general, because the west of the Osaka Plain is Osaka bay and the eastern part of it faces the mountains They are also different from the sections for the initial models.

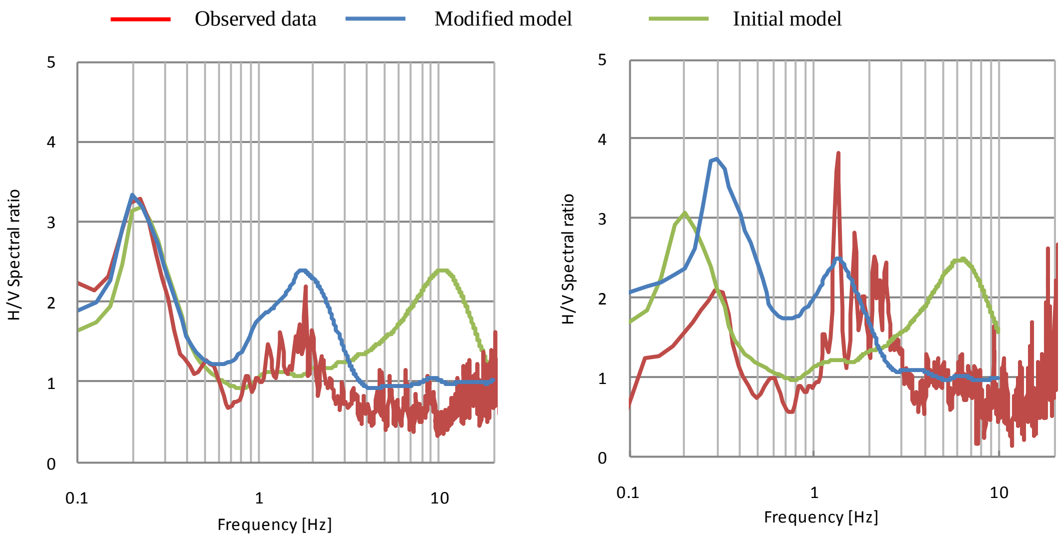

(a) osk2-11 (b) osk1-4

Figure 5.1. Comparison of H/V spectral ratios for observed data, initial model, and modified model for points (a) osk2-11, (b) osk1-4. For the observed, either NS/UD or EW/UD spectral ratio is selected for comparison

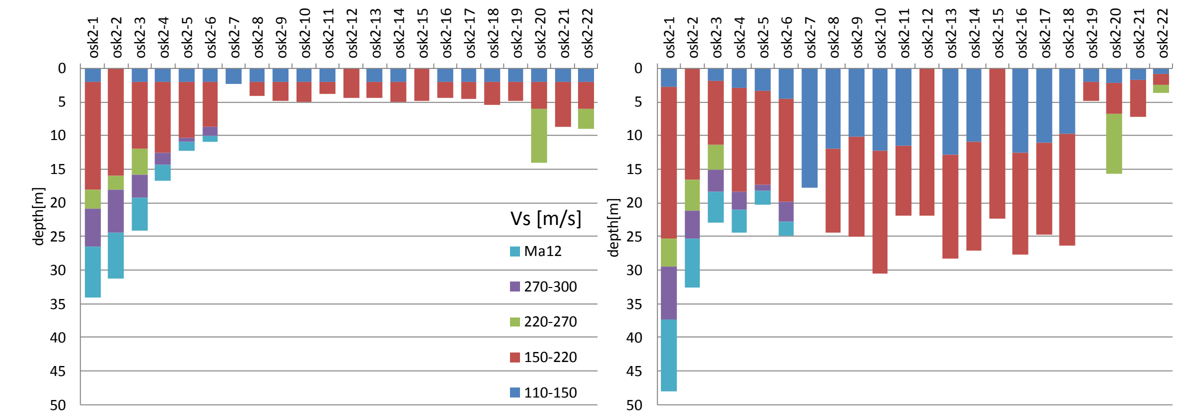

(a) Initial model (b) Modified model

Figure 5.2. Sections of the shallower subsurface structures of the (a) initial and (b) modified models of Line 2

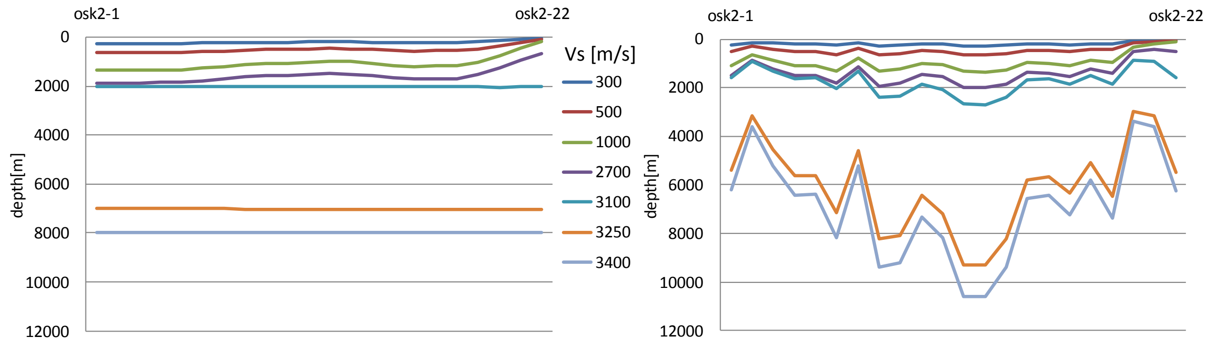

(a) Initial model (b) Modified model

Figure 5.3. Sections of the deeper subsurface structures of the (a) initial and (b) modified models of Line 2

These differences as shown in Figs. 5.1 to 5.3 can be result of following two points. First is that we could not get precise data by noise and some particular effect in the mountains around the eastern edges of Lines 1 and 2. Second is that in the identification, the procedure to change the whole layer thickness of the initial model is may be too oversimplified. So next we paid attention to changing both thickness and velocity structures of underground models.

Secondly we identified both thickness and velocity structures of underground layers together. We changed only velocities for shallower underground structures consisting of 2 to 9 layers and both thickness and velocity for three upper layers of deeper underground structures consisting 7 layers. In identification we used the least-squares method and indentified modified underground structures which give minimum error between H/V spectral ratios gained from microtremor measurements and theoretical calculation of modified underground structure models.

Fig. 5.4 shows comparison of H/V spectral ratios for observed data, initial model, and two modified models using the different identification approaches for osk1-18. One of the two modified models is followed by 1/4 wavelength law and the other is followed by the least-squares method. Although we can see no obvious difference between H/V spectral ratios for the two modified models, H/V spectral ratio for latter modified model seems to match better with that for observed data.

In order to make sure that our identification approach using the least-squares method is more appropriate, Fig. 5.5 shows comparison of S-wave velocity structure for initial and the two modified models for osk1-18. While the modified S-wave velocity structure based on 1/4 wavelength law is changed dramatically from the initial one, anther modified S-wave velocity structure using least-squares method has some preferable modification from initial one.

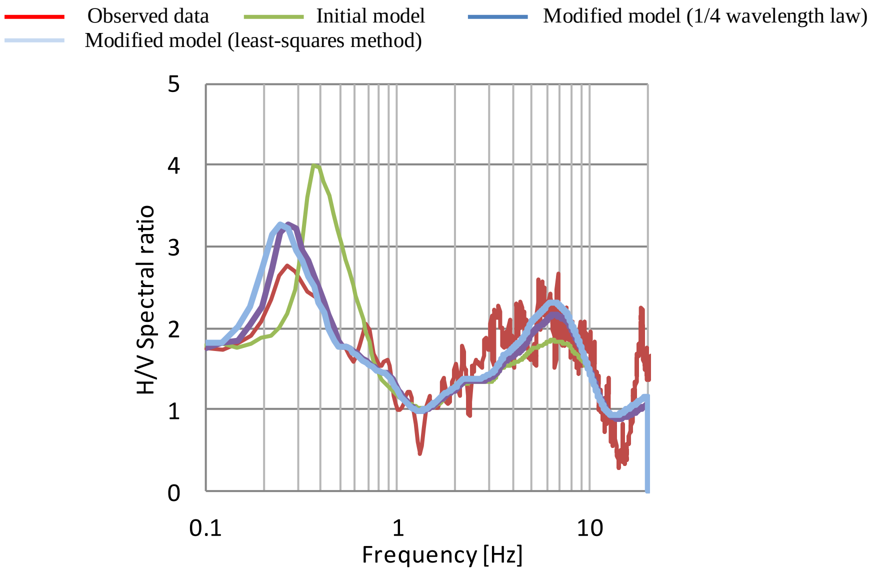

Figure 5.4. Comparison of H/V spectral ratios for observed data, initial model, and two modified models for osk1-18. One of the two modified models is followed by 1/4 wavelength law and the other is followed by the least-squares method

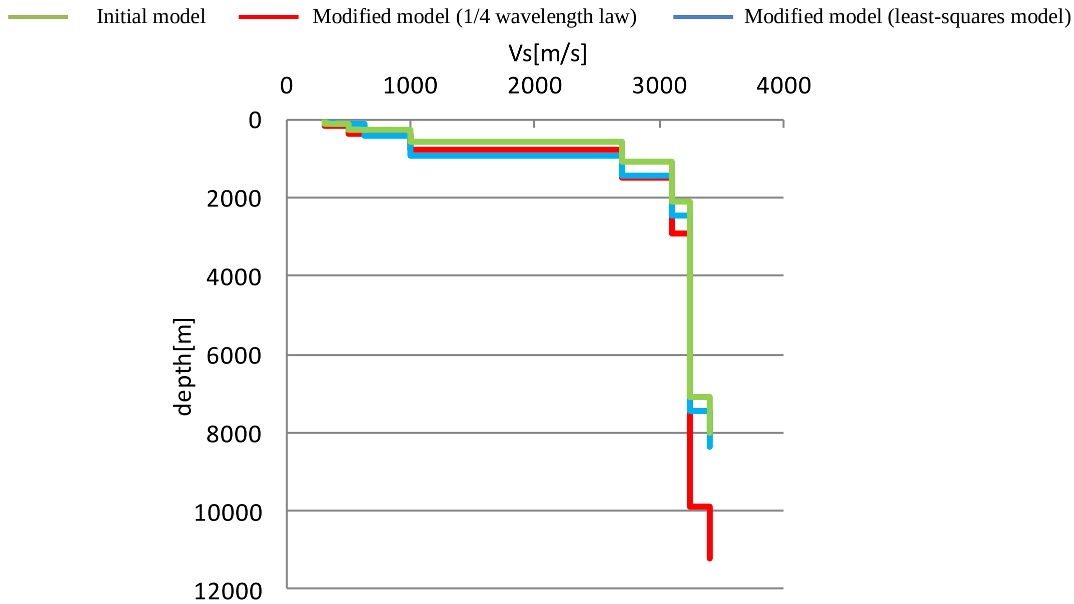

Figure 5.5. Comparison of S-wave velocity structures for initial model and two modified models for osk1-18

6. DISCUSSIONS AND CONCLUSIONS

We observed microtremors at 44 points along two liner lines and three strong ground motion stations in the southern part of the Osaka Plain in Japan. By comparing H/V spectral ratios calculated from microtremor measurements with theoretical calculation and searching for the better 1-D structure at each site based on predominant frequencies and amplitudes at these predominant frequencies of the H/V spectral ratio, we estimated underground structures and found that our identification approach where we change both thickness and velocity of an underground structure together using the least-squares method was appropriate. We are planning to estimate underground structures at all observation stations along the two lines and study the results in detail. In addition, we would like to estimate strong ground motion in the southern part of the Osaka Plain extensively with high precision by combining our estimated underground structures and source models of previously proposed studies together.

ACKNOWLEDGEMENT

The authors greatly appreciate Dr. Sánchez-Sesma for the use of his code to calculate theoretical H/V spectral ratio of microtremors. Soil property data of J-SHIS, AIST, and those from K-NET and KiK-net loggings are also highly appreciated. This research was partially supported by JSPS and NSF under the Japan-U.S. Cooperative Science Program from 2011~2012 (P.I. Hiroshi Kawase, DPRI, Kyoto Univ.) and MEXT Grant-in-Aid for Scientific Research (A) No.21241044, 2009~2012 (P.I. Hiroshi Kawase, DPRI, Kyoto Univ.).

REFERENCES

Aoi, S., K, Obara., S, Hori., K, Kasahara. and Y, Okada. (2000). New strong-motion observation network: KiK-net. Eos Trans. AGU, 81(48), Fall Meet. Suppl., Abstract S71A-05.

Japan Seismic Hazard Information Station. http://www.j-shis.bosai.go.jp/. 2011/7/15

Kinoshita, S. (1998). Kyoshin Net (K-NET). Seism. Res. Lett. 69. pp. 309-332.

Sánchez-Sesma F. J., J. A. Pérez-Ruiz, F. Luzón, M. Campillo, and A. Rodoríguez-Castellanos. (2008). Diffuse fields in dynamic elasticity. Wave Motion, 45. pp.641-654

Sánchez-Sesma, F. J., M. Rodríguez, U. Iturrarán-Viveros, F. Luzón, M. Campillo, L. Margerin, A. García-Jerez, M. Suarez, M. A. Santoyo, A., and Rodríguez- Castellanos. (2011). A theory for microtremor H/V spectral ratio: Application for a layered medium. Geophys. J. Int. Exp. Lett., In press, doi: 10.1111/j.1365-246X.2011.05064.x.

Sekiguchi, H., N. Kitada, H. Ito, and Y. Sugiyama. (2005). PS and density logging in a 300 m borehole at Nakanoshima in Kita Ward, Osaka City. Annual Report on Active Fault and Paleoearthquake Researches, No. 5, pp. 109-113.

Yoshida, K., H, Sekiguchi. and K, Yamamoto. (2010). Shallow structure model of the Osaka sedimentary basin CD-ROM. *Geological Survey of Japan Interim Report no. 52*. Geological Survey of Japan. National Institute of Advanced Industrial Science and Technology.